Optics Letters

Evanescent point sources: application to microsphere-assisted super-resolution microscopy

Rayenne Boudoukha,[1,2] Stéphane Perrin,[1,3] Assia Guessoum,[4] Nacer-E. Demagh,[2,4] Paul Montgomery,[1] and Sylvain Lecler[1,5,*]

[1]ICube Research Institute, Université de Strasbourg - INSA Strasbourg - CNRS, Strasbourg 67000, France
[2]Applied Optics Laboratory, Institute of Optics and Precision Mechanics, Ferhat Abbas University Setif1, Setif, Algeria
[3]Photonics Bretagne, Lannion 22300, France
[4]Laboratoire d'Electronique Quantique, Faculté de Physique, USTHB, Algiers, Algeria
[5]INSA Strasbourg, Strasbourg 67000, France
*sylvain.lecler@insa-strasbourg.fr

Received 25 September 2024; revised 17 October 2024; accepted 22 October 2024; posted 22 October 2024; published 5 November 2024

In the rigorous electromagnetic simulation of an imaging system, the evanescent waves from a point source or from a sample are naturally mixed with the propagative waves. Therefore, their contributions are difficult to distinguish. We present a point-source model made of only the evanescent waves. To illustrate its potential, the model is applied to the study of the evanescent-wave contribution in microsphere-assisted microscopy (MAM). The contribution of the evanescent waves in the microsphere imaging process is clearly demonstrated. However, we also show that this contribution is not enough to justify the super-resolution. The destructive interference between two close point sources may be the key physical phenomenon.

https://doi.org/10.1364/OL.542794

The relevant numerical tools to investigate the performance of an imaging system depend on the size, the aperture, and the working distance of the optical elements. In the paraxial hypotheses, when the diameter of lenses is larger than the wavelength or the aperture is smaller, or when the image is in the far field, ray-tracing methods appear to be well-adapted [1]. Fourier optics can be used to include the wave nature of light in the imaging process, e.g., to estimate the point spread function or to simulate diffractive optical elements [2]. However, rigorous vectorial electromagnetic simulations are required for smaller optical elements, larger numerical aperture, or smaller working distances. In this case, Maxwell equations or the vectorial propagation theory is thus needed. Moreover, the propagation of the evanescent waves must be included in the propagation process when the distance between the object plane and the lens is comparable to the wavelength of light, such as in microsphere-assisted microscopy (MAM) [3,4]. In MAM [5], as well as in scanning near-field optical microscopy [6], solid immersion microscopy [7], and imaging using superlenses and hyperlenses [8], the evanescent waves are converted into propagative waves and contribute to the image in the far field. Compared to the SNOM or to the PALM/STORM techniques [9,10], MAM is a full-field label-free imaging technique, enabling to achieve a sub-diffraction-limit resolving power [11]. A dielectric microsphere placed at a distance smaller than 1 μm from the sample provides a magnified virtual image with a resolution of $\lambda/5$ in air and $\lambda/7$ in immersion [12,13]. A classical microscope lens or ball-lens collects then the image [14]. However, if its resolving power has been experimentally demonstrated in 2011 by Wang *et al.* [12], the physical understanding is up to now not clearly defined. Several models and concepts have been proposed such as the ability of a dielectric micro-particle to generate a photonic jet (PJ). This is a beam focused by the microsphere beyond the diffraction limit at the mesoscale. However, the PJ width is larger than the experimentally reached resolutions [15,16]. The role of whispering-gallery mode resonances within the microspheres has also been studied [17]. But the numerical demonstration was performed by implementing two point sources without indicating the specific contribution of the evanescent waves from the point sources to the image formation. The ability of the microspheres to convert evanescent in propagative waves [18], deduced from experimental observations [19,20], has been theoretically demonstrated in 2021 [5]. However, the complete description of the imaging process was missing. Finally, the role of coherence in the imaging process has been pointed out where two point objects need to be out of phase in order to be resolved [21]. In the theoretical investigations of the imaging process mentioned before, rigorous electromagnetic simulations have been used with two families of method to describe the object: (1) using direct point sources (generally oscillating dipoles) and (2) considering secondary sources, which are the real objects illuminated by a classical source (plane wave, focused wave, or Khöler source). However, an important limitation of these techniques is that they do not allow the separation of the contributions of the evanescent waves and the propagative ones. While a super-resolved image has been predicted, the underlying physical phenomenon has not necessarily been identified.

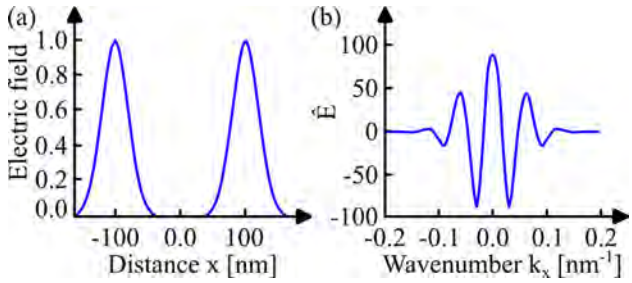

Fig. 1. Theoretical description of the electric field of two evanescent point sources. (a) Amplitude of the electric field $E(x)$ of the two point sources in the object plane ($y = 0$ µm). (b) Frequency-domain decomposition of $E(x)$ as a function of the wavenumber k_x.

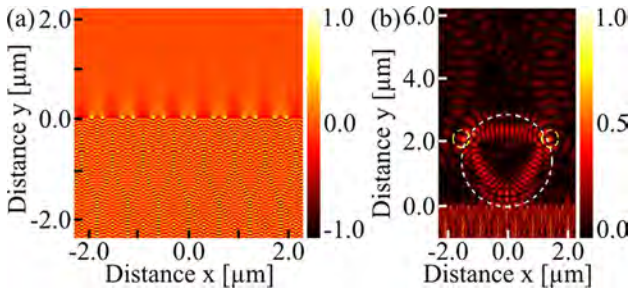

Fig. 2. (a) Electric field E_z of the evanescent point sources obtained by summation of the total internal reflections. (b) $|E_z|$, interaction of the evanescent point sources in phase with a 3 µm microsphere ($n_2 = 1.5$). $\lambda_0 = 600$ nm. The microsphere is illustrated in a white dashed line.

In this work, we propose a new kind of source: the evanescent point source where the point source is only composed of evanescent-wave components. Applied to helping in the understanding of the imaging process of MAM, we show that while a microsphere is able to image such an evanescent point source, unfortunately it is not sufficient to explain the super-resolution. The destructive interference between the images of two close point sources, possibly due to the short optical path differences involved, seems to be the main explanation. This evanescent point-source model opens new possibilities to investigate many other micro-systems for applications from imaging to a sensor.

The model of the evanescent point source is defined in two dimensions in the (0, x, y) plane. The object plane lies in the x-direction at $y = 0$ µm and the wave is evanescent in the y-direction, with k_y an imaginary number. The wavenumber along the x-direction can thus be defined as $k_x = \sqrt{k_0^2 - k_y^2}$, with $k_x > k_0$ corresponding to high spatial frequencies in the object plane. In optical imaging, these spatial frequencies correspond to the details to resolve.

In our model, the free space wavelength is $\lambda_0 = 600$ nm, and the two in-phase point sources are separated by a distance d smaller than half a wavelength ($d = 200$ nm). Their half-width at 1/e of the electric field norm is $W = 50$ nm as illustrated in Fig. 1(a). The electric field along the x-direction is given by Eq. (1):

$$E(x) = E_0 \exp\left(\frac{-x^2}{W^2}\right) * (\delta(x - d/2) + \delta(x + d/2)), \quad \textbf{(1)}$$

where $\delta(x)$ is the Dirac distribution. In the frequency domain, the electric field $\hat{E}(x)$ is retrieved by the Fourier transform the $E(x)$ (Eq. (2)), and the corresponding angular spatial frequencies are shown in Fig. 1(b):

$$\hat{E}(k_x) = 2\sqrt{\pi} W E_0 \exp(-W^2 k_x^2/4) \cos(k_x d/2). \quad \textbf{(2)}$$

The k_x axis has been divided into 19 $k_{x,n}$ values (= 2P+1, with P = 9) from −0.1 nm^{-1} to 0.1 nm^{-1} by a step $\Delta k_x = 0.1/9$ nm^{-1}/P. The point sources may be ideally generated by summing these 19 waves, each one having an amplitude $\hat{E}(k_{x,n})$. Most of these waves, when $k_x > 2\pi/\lambda_0$ ($k_x > 0.01047$ nm^{-1}), are evanescent in the y-direction.

These evanescent waves can be obtained by total internal reflection, using a dielectric substrate with a high refractive index ($n = 10$) placed under the object plane. To generate an evanescent wave having a tangential vector k_x, a plane wave with an incident angle $\theta_i = asin(k_x/(k_o \times n))$ can be used. The angle θ_i must be larger than the critical angle $\theta_c = asin(1/n)$, reaching, in our case, $\theta_c = 5°$. The normal vector $k_x = 0$ nm^{-1} (corresponding to $\theta_c = 0°$), the only one that would correspond to a propagative wave is removed.

Periodic pairs of point sources along the x axis, as well as the superposition of the total internal reflections, are shown in Fig. 2(a). The period between two evanescent point sources is determined by the sampling in the frequency domain k_x. The resulting wave is stationary along the x-direction and the evanescent wave along the y-direction. Compared to oscillating dipoles, light does not propagate in the y-direction. Out-of-phase point sources can also be considered where their electric field is given by Eq. (3) and their angular spatial spectrum by Eq. (4):

$$E(x) = E_0 \exp\left(\frac{-x^2}{W^2}\right) * (\delta(x - d/2) - \delta(x + d/2)), \quad \textbf{(3)}$$

$$\hat{E}(k_x) = 2i\sqrt{\pi} W E_0 \exp(-W^2 k_x^2/4) \sin(k_x d/2). \quad \textbf{(4)}$$

The imaging process in MAM is investigated using this new model of evanescent point sources. A 3-µm-diameter microsphere with a refractive index of 1.5 is introduced above the two point sources. Figure 2(b) shows the electric field norm $|E|$. The light emanating from the point sources is coupled inside the microsphere. This coupling has already been studied in Ref. [5]. Internal reflections appear inside the sphere and create an internal stationary state. Moreover, outgoing waves propagate in the far field, confirming the ability of a microsphere to convert evanescent waves into propagating waves. In Fig. 2(b), two maxima of intensity can be observed near the top of the microsphere which could initially be interpreted as a real image of the point sources. However, when a translation of the two point sources in the object plane is implemented, the two maxima do not experience an equivalent translation (taking into account the magnification) in the image-like plane. In reality, the image is virtual. In order to simulate the virtual image generation, the following trick can be used: the outgoing wave is captured at the top of the simulation windows and, then, used in a time-reversal propagation in free space without the microsphere, nor the substrate, as explained in Ref. [21]. Figure 3(a) shows the virtual image of the two in-phase evanescent point sources through the microsphere. Only one image feature appears. The two points are thus not resolved despite the contribution of the evanescent waves. A similar result is observed in Fig. 3(c) when classical in-phase point sources (i.e., two dipoles) are imaged. This numerical analysis shows that the origin of the

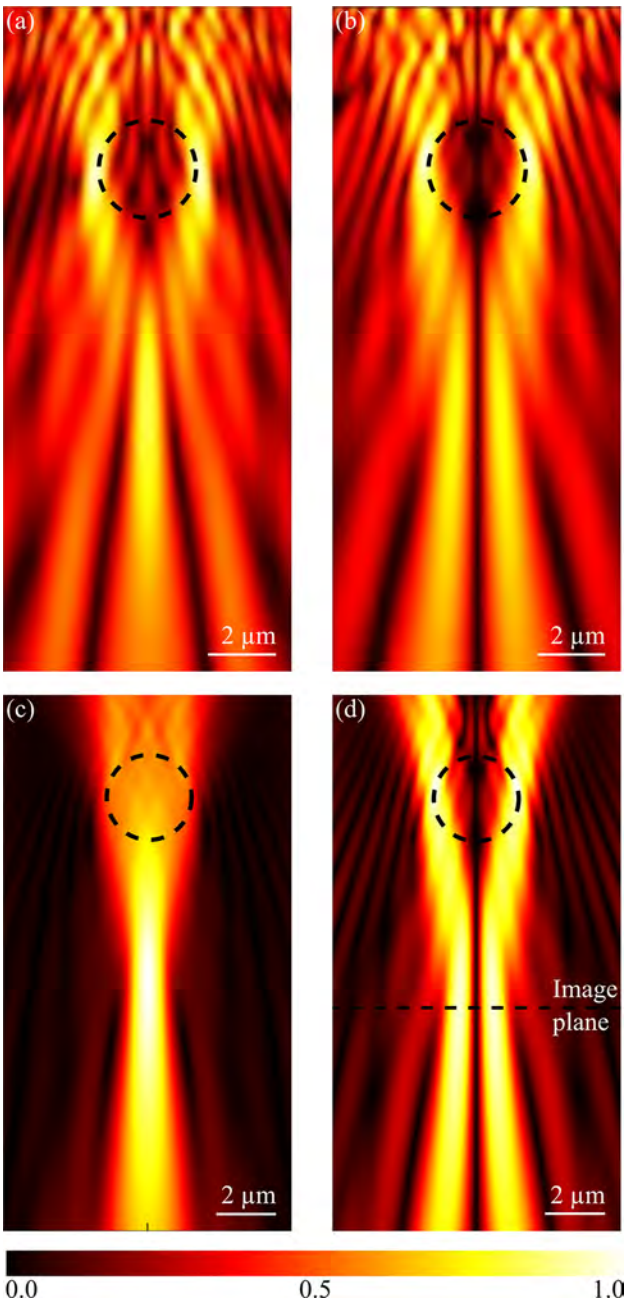

Fig. 3. Backpropagation of the electric field from two point sources by using the time-reversal propagation algorithm. Evanescent point sources are (a) in phase and (b) out of phase. Classical point sources (oscillating dipoles) are (c) in phase and (d) out of phase. The image plane is illustrated in a black-dashed line.

super-resolution phenomenon cannot be explained only by the evanescent contribution of the object.

On the other hand, Figs. 3(b) and 3(d) show the virtual images from two out-of-phase evanescent source and classical sources, respectively. Two distinct images of points appear. The features of the object are resolved by the microsphere due to the destructive interference between their images. A profile of the intensity in the image plane for the out-of-phase evanescent point sources (Fig. 3(b)) is shown in Fig. 4.

This work presents the concept of evanescent point sources and its numerical implementation. The size of each source and

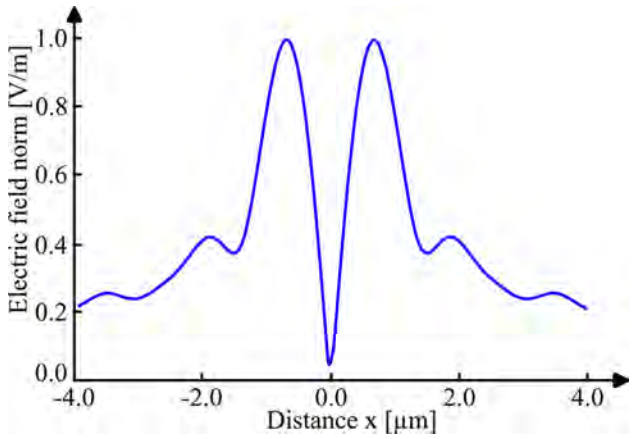

Fig. 4. Norm of the electric field $E(x)$ in the virtual image plane (Fig. 3(d)).

the distance between them are smaller than half a wavelength. Generated in the object plane by summing the total internal reflections, these sources do not have any wave propagation in the far field, compared with classical oscillating dipoles. Using these sources, we have investigated the imaging process of microsphere-assisted microscopy. The ability of the microspheres to convert evanescent waves into propagating waves in the far field is confirmed as demonstrated in Ref. [5]. Moreover, their ability to image the evanescent point sources is demonstrated for the first time. However, this phenomenon appears to be insufficient to justify the super-resolution imaging. Indeed, only the out-of-phase point sources are resolved. The super-resolution phenomenon through the microspheres may be therefore due to the phase difference along the object plane, as suggested in Ref. [22]. Interference may also be experimentally possible despite the low coherence source used in the experimental setup. In reality, the coherence of light must be lower than the optical path difference and the small size of the microspheres. These observations are in good agreement with the recent paper of Maslov [22] where the sub-diffraction-limit phenomenon was demonstrated only considering the coherence of light. Maslov has also shown that the total internal reflections inside the microsphere (also named whispering-gallery mode), excited by the evanescent waves from the object, contribute not by their far-field conversion but by their re-illumination of the object. Moreover, as has been demonstrated for several microscopy techniques, when the imaging is applied close or beyond the diffraction limit, the resolution estimation also depends on the material properties and on the applied estimation technique (PSF, MTF, etc.) [13,23].

Funding. Campus France (19MDU217); Société d'Accélération du Transfert de Technologies (Conectus, Projet Nano3D); Conseil Régional du Grand Est (FRCR Mirage).

Disclosures. The authors declare no conflicts of interests.

Data availability. Data underlying the results presented in this paper are not publicly available at this time but may be obtained from the authors upon reasonable request.

REFERENCES

1. M. Born and E. Wolf, *Principles of Optics*, 7th ed. (Cambridge University Press, 1999).

2. P. Duffieux, *The Fourier Transform and Its Applications to Optics* (John Wiley & Sons, 1983).
3. T. Pahl, L. Hüser, S. Hagemeier, *et al.*, Light: Adv. Manuf. **3**, 699 (2022).
4. A. Maslov and A. Erykalin, Appl. Opt. **63**, 1282 (2024).
5. R. Boudoukha, S. Perrin, A. Demagh, *et al.*, Photonics **8**, 73 (2021).
6. D. Pohl and D. Courjon, *Near Field Optics* (Springer, 1993).
7. N. V. Chernomyrdin, M. Skorobogatiy, D. S. Ponomarev, *et al.*, Appl. Phys. Lett. **120**, 110501 (2022).
8. D. Smith, D. Schurig, M. Rosenbluth, *et al.*, Appl. Phys. Lett. **82**, 1506 (2003).
9. S. Hell and J. Wichmann, Opt. Lett. **19**, 780 (1994).
10. E. Betzig, G. Patterson, R. Sougrat, *et al.*, Science **313**, 1642 (2006).
11. V. N. Astratov, Y. B. Sahel, Y. C. Eldar, *et al.*, Laser Photonics Rev. **17**, 031102 (2023).
12. Z. Wang, W. Guo, L. Li, *et al.*, Nat. Commun. **2**, 218 (2011).
13. A. Darafsheh, J. Appl. Phys. **131**, 031102 (2022).
14. S. Perrin, R. Pierron, P. Gerard, *et al.*, Appl. Phys. Lett. **122**, 161108 (2023).
15. S. Lecler, S. Perrin, A. Leong-Hoi, *et al.*, Sci. Rep. **9**, 4725 (2019).
16. A. Maslov and V. Astratov, Phys. Rev. Appl. **11**, 064004 (2019).
17. S. Zhou, Y. Deng, W. Zhou, *et al.*, Appl. Phys. B **123**, 236 (2017).
18. Y. Ben-Aryeh, J. Opt. Soc. Am. A **33**, 2284 (2016).
19. Q. Lin, D. Wang, Y. Wang, *et al.*, Opt. Quantum Electron. **48**, 557 (2016).
20. S. Yang, Y.-H. Ye, Q. Shi, *et al.*, J. Phys. Chem. C **124**, 25951 (2020).
21. I. Kassamakov, S. Lecler, A. Nolvi, *et al.*, Sci. Rep. **7**, 3683 (2017).
22. A. Maslov and V. Astratov, Appl. Phys. Lett. **124**, 061105 (2024).
23. V. A. Zhelnov, N. V. Chernomyrdin, G. M. Katyba, *et al.*, Adv. Opt. Mater. **12**, 2300927 (2024).